Hindawi
Applied and Environmental Soil Science
Volume 2021, Article ID 6617541, 15 pages
https://doi.org/10.1155/2021/6617541

Research Article

Land Use/Land Cover Change Impact on Hydrological Process in the Upper Baro Basin, Ethiopia

Tewodros Getu Engida,[1] **Tewodros Assefa Nigussie**,[2] **Abreham Berta Aneseyee**,[3] **and John Barnabas**[4]

[1]*Gambella University, College of Engineering and Technology, Department of Water Resource and Irrigation Engineering, Gambela, Ethiopia*
[2]*Institute of Technology, Hawassa University, Awassa, Ethiopia*
[3]*Wolkite University, Department of Natural Resource Management, P. O. Box No: 07, Wolkite, Ethiopia*
[4]*Gambella University, College of Agriculture and Natural Resource Management, Department of Plant Science, P.O. Box 126, Gambella, Ethiopia*

Correspondence should be addressed to John Barnabas; johnbarnabas@gmail.com

Received 17 December 2020; Revised 30 June 2021; Accepted 17 July 2021; Published 29 July 2021

Academic Editor: Evgeny Abakumov

Understanding the hydrological process associated with Land Use/Land Cover (LU/LC) change is vital for decision-makers in improving human wellbeing. LU/LC change significantly affects the hydrology of the landscape, caused by anthropogenic activities. The scope of this study is to investigate the impact of LU/LC change on the hydrological process of Upper Baro Basin for the years 1987, 2002, and 2017. The Soil Water Assessment Tool (SWAT) model was used for the simulation of the streamflow. The required data for the SWAT model are soils obtained from the Food and Agriculture Organization; Digital Elevation Model (DEM) and LU/LC were obtained from the United States Geological Survey (USGS). The meteorological data such as Rainfall, Temperature, Sunshine, Humidity, and Wind Speeds were obtained from the Ethiopian National Meteorological Agency. Data on discharge were obtained from Ministry of Water, Irrigation and Electricity. Ecosystems are deemed vital. Landsat images were used to classify the LU/LC pattern using ERDAS Imagine 2014 software and the LU/LC were classified using the Maximum Likelihood Algorithm of Supervised Classification. The Sequential Uncertainty Fitting (SUFI-2) global sensitivity method within SWAT Calibration and Uncertainty Procedures (SWAT-CUP) was used to identify the most sensitive streamflow parameters. The calibration was carried out using observed streamflow data from 01 January 1990 to 31 December 2002 and a validation period from 01 January 2003 to 31 December 2009. LU/LC analysis shows that there was a drastic decrease of grassland by 15.64% and shrubland by 9.56% while an increase of agricultural land and settlement by 18.01% and 13.01%, respectively, for 30 years. The evaluation of the SWAT model presented that the annual surface runoff increased by 43.53 mm, groundwater flow declined by 27.58 mm, and lateral flow declined by 5.63 mm. The model results showed that the streamflow characteristics changed due to the LU/LC change during the study periods 1987–2017 such as change of flood frequency, increased peak flows, base flow, soil erosion, and annual mean discharge. Curve number, an available water capacity of the soil layer, and soil evaporation composition factor were the most sensitive parameters identified for the streamflow. Both the calibration and validation results disclosed a good agreement between measured and simulated streamflow. The performance of the model statistical test shows the coefficient of determination (R^2) and Nash–Sutcliffe (NS) efficiency values 0.87 and 0.81 for calibration periods of 1990–2002 and 0.84 and 0.76 for the validation period of 2003 to 2009, respectively. Overall, LU/LC significantly affected the hydrological condition of the watershed. Therefore, different conservation strategies to maintain the stability and resilience of the ecosystem are vital.

1. Introduction

The response of hydrologic circulation is closely related to land use planning and management [1, 2]. Land Use/Land Cover (LU/LC) change is one of the factors that directly affect the watershed hydrological cycle [3–5]. It has been widely accepted that human activities cause LU/LC change and have imposed a great impact on the hydrological processes and water resources of the watershed [6] For example, a study [1] showed that the water provision and the hydrological process decreased as consequence LU/LC change that was aggravated by significant increasing population pressure and development in Pennar Basin in India. This can be either by increasing the water yield or by eliminating the flow in some circumstances, thereby increasing the sediment load and decreasing the groundwater [7, 8].

LU/LC changes and population growth are the most common problems in developing countries such as Ethiopia since their economic development mainly depends on agriculture [9]. In the past 40 years, the increases in human activities resulted in the expansion of agricultural land, extraction of timber, and urbanization, thereby resulting in deforestation in southwest Ethiopia [10, 11], while these changes in land cover affect the local watershed hydrological cycle and flood vulnerability of various subwatersheds [12]. The modifications/conversions of natural vegetation and physical soil conditions are usually the principal cause of changes in rainfall-runoff characteristics of the local catchment, which consequently change the river flow regimes [13, 14]. Several studies show that the changes in vegetation cover, i.e., deforestation, lead to an increase in water yield and sedimentation [15, 16].

Watershed studies can provide direct evidence of LU/LC change impacts on runoff [17]. For these reasons, hydrological models are becoming important for studying LU/LC change effect on the hydrological cycle in a landscape [18, 19]. Several studies were carried out on the hydrology of the watershed by utilizing LU/LC data in different regions of Ethiopia using the Soil and Water Assessment Tool (SWAT). They indicated an increase in the wet seasonal flow, surface runoff, and water yield [20–23]. However, studies on the impact of the LU/LC dynamic on the hydrology regime of the Upper Baro Basin are limited.

The Upper Baro Basin is hurt from human-induced degradation mainly due to large-scale agricultural expansion, which leads to LU/LC dynamism. The impacts of such changes on local hydrology are poorly understood. Hence, systematic analyses and understanding the impacts of LU/LC changes on the watershed hydrology are important for planning water resources management and maintaining the sustainable flow of water to the Baro-Akobo River. This study also helps decision-makers know where to invest to conserve the hydrological services.

Therefore, the objectives of the study are as follows: (1) to assess the LU/LC change over the past 30 years on the hydrological response of Upper Baro Basin and (2) to check the applicability of SWAT model for the study area.

2. Materials and Methods

2.1. The Study Area. The Upper Baro Basin is found in southwestern Ethiopia located at 766 km away from Addis Ababa, the capital city of Ethiopia, between latitudes 7.44° and 9.41°N and longitudes 34.52° and 36.31°E, covering an area of 23462 km^2. The altitude ranged from 390 m to 3266 m above sea level (Figure 1).

The Upper Baro basin has a long rainy season in the months of May-September. The area indicates a monomodal, bimodal, and triple-modal rainfall pattern. The annual average rainfall is varying from about 1163.03 mm to over 2258.36 mm with a monthly maximum rainfall record of 302.79 mm in August, while relative mean monthly rainfall for dry seasons occurs between December and March (Figure 2).

The annual rainfalls show pronounced annual and seasonal fluctuations (Figure 3) and the maximum temperature of Upper Baro Basin ranges between 27.7°C (in the wet season) and 37.2°C (in the dry season) and occurs in June to August, while the minimum falls between 10.8°C and 13.7°C in the year.

The topography of the Upper Baro Basin is characterized by variation from flat to mountainous terrain and falls in the altitude range of 390 m to over 3000 m a.m.s.l. with 42% in between 1000 m and 2000 m a.m.s.l. The eastern two-thirds of the basin area lies between 1000 m and 2400 m a.m.s.l. and a gently sloping plain lies in the west between 380 m and 500 m a.m.s.l. Dystric nitisols and dystric gleysols are the dominant soil type in the study area.

2.2. SWAT Model Data Types and Analysis

2.2.1. Meteorological Data. The SWAT model requires daily meteorological (Weather) data such as daily precipitation, minimum and maximum air temperature, relative humidity, wind speed, dew point, and daily sunshine. The standard deviation of each parameter was calculated. Thiessen method is used to adjust for nonuniform meteorological station distribution by proportion to the area which is closer. Eleven meteorological stations were selected (Table 1) based on the quantity, quality, period, consistency, homogeneity, and their uniform distribution within and around the Upper Baro Basin. These data were obtained from the National Meteorological Agency of Ethiopia (NMAE) over the period (1987–2017). The missing values were estimated from other stations around the missed record station by using both arithmetic mean method and normal ratio method and also consistency test which shows double mass.

The SWAT weather generator model (WGEN) was used to match the access table and lookup table. The daily precipitation and temperature of all gauging stations were prepared in comma-delimited (.csv) format. Solar radiation, relative humidity, and wind speed data were available only for principal Gore and Masha stations (synoptic stations).

2.2.2. Soil Data. Seventy soil types have been identified at Upper Baro Basin (Table 2). The spatial soil data were obtained from the Ethiopian Ministry of Water, Irrigation, and

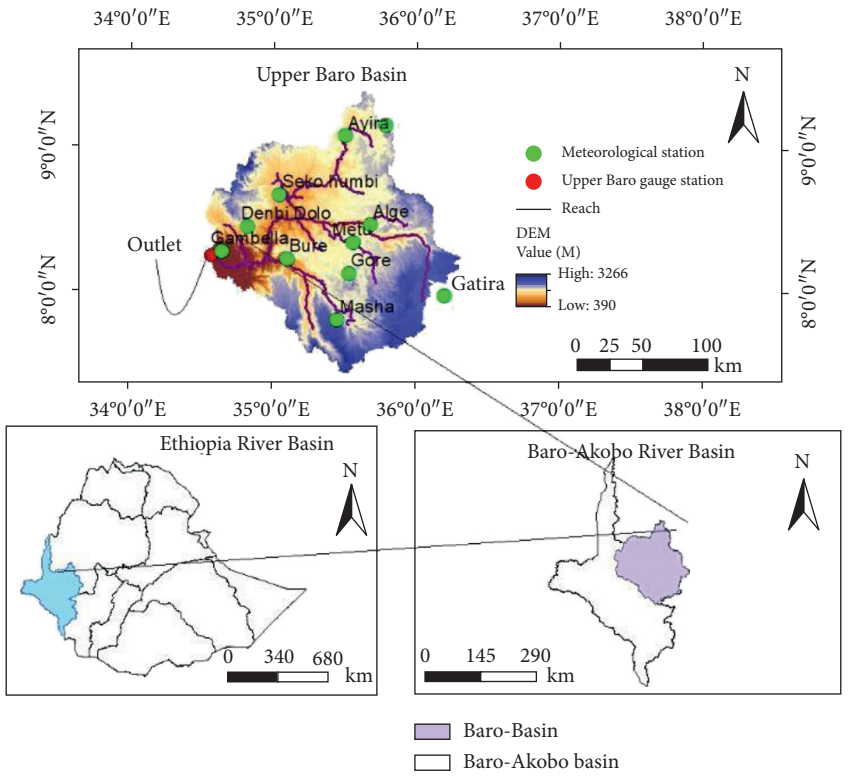

Figure 1: Map of the study area.

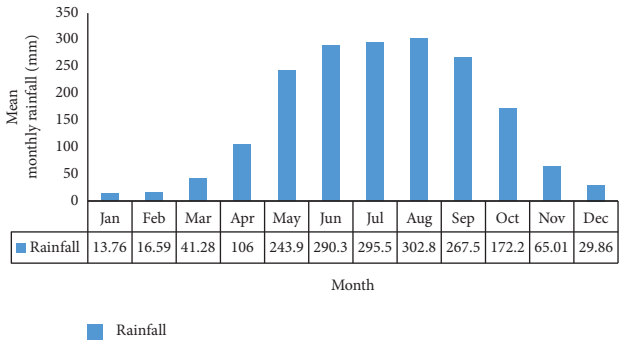

Figure 2: Average monthly areal rainfall distribution throughout 1987–2017.

Electricity (MWIE), which is prepared according to FAO soil classification. The most dominant soil in the basin is Dystric nitisols and Dystric gleysols.

SWAT model requires physical and chemical soil properties in the simulation of a hydrological component such as available water content, soil texture, hydraulic conductivity, bulk density, and organic carbon content for the different layers of each soil type where shown. The major soils of the Upper Baro Basin are as shown below table and a lookup table was prepared for each type of soil.

2.2.3. DEM. DEM with a resolution of 30 m was downloaded from United States Geological Survey https://earthexplorer.usgs.gov/. The DEM is one of the essential inputs required by SWAT to delineate Upper Baro

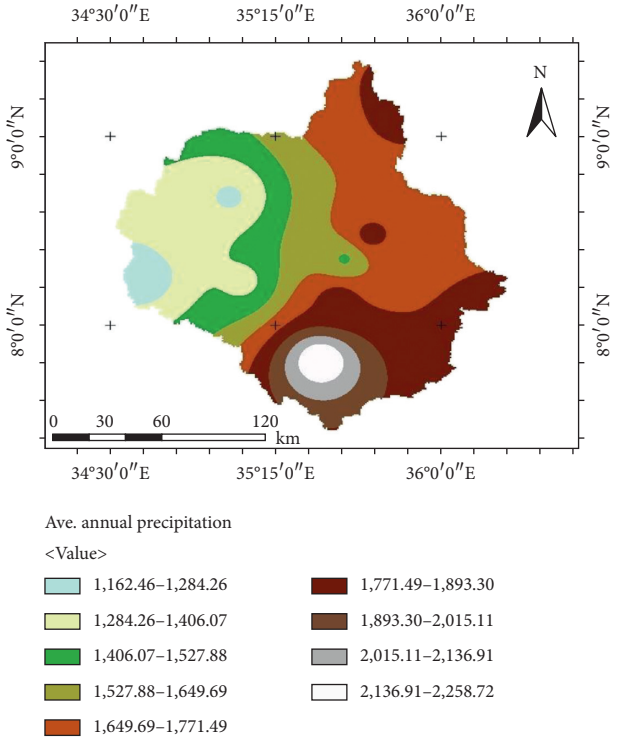

Figure 3: Annual areal rainfall distribution (mm) for the period of 1987–2017.

Basin (Figure 4), define the stream network, and determine sub-basin parameters such as slope area and slope length.

Table 1: Summary of the meteorological stations.

Station	Coordinate		Altitude (m)	Station class	Period of data
	Longitude	Latitude			
Gambella	34.5833	8.25	430	C2	1983–2017
Mettu	35.56667	8.2833	1711	C2	1981–2017
Dembi Dolo	34.8	8.5167	1850	C2	1982–2017
Ayira	35.55	9.1	1555	C2	1987–2017
Gatira	36.2	7.983	2358	C2	1987–2017
Masha	35.4667	7.75	2282	C1	1981–2017
Gore	35.5333	8.1333	2033	C1	1981–2017
Seko Humbi	34.9833	8.7166	1860	C2	1987–2017
Gimbi	35.7833	9.1666	1970	C2	1983–2017
Bure	35.1	8.2333	1750	C2	1981–2017
Alge	35.6667	8.5333	1880	C2	1987–2017

Table 2: Soil type's area coverage and SWAT code.

Value	Soil types	Area (km^2)	Area covered (%)	SWAT code
1	Dystric nitisols	14151.76	60.32	DYNITISOLS
2	Dystric gleysols	5423.52	23.12	DYGLEYSOLS
3	Orthic acrisols	326.87	1.39	ACRISOLS
4	Chromic luvisols	120.45	0.51	CHLUVISOLS
5	Orthic solonchaks	778.06	3.32	SOLONCHAKS
6	Calcic xerosols	363.20	1.55	CLXEROSOLS
7	Leptosols	255.95	1.09	LEPTOSOLS
8	Iatric cambisols	1041.60	4.44	EUCAMBISOLS
9	Eutric nitisols	108.43	0.46	EUNITISOLS
10	Eutric fluvisols	276.99	1.18	EUFLUVISOLS
11	Dystric cambisols	58.40	0.25	DYCAMBISOLS
12	Gypsic yermosols	43.39	0.18	GYYERMOSOLS
13	Dystric fluvisols	231.44	0.99	DYFLUVISOLS
14	Cambisols	2.54	0.01	CAMBISOLS
15	Calcic fluvisols	92.40	0.39	CLFLUVISOLS
16	Calcic cambisols	167.83	0.72	CLCAMBISOLS
17	Calcaric flubisols	19.17	0.08	CLFLUBISOLS

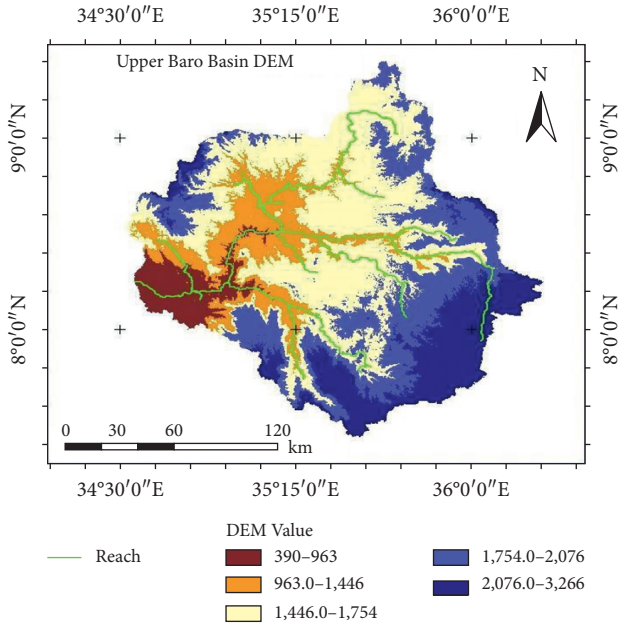

Figure 4: DEM map (meters a.m.s.l.) of Upper Baro Basin.

2.2.4. Slope Classes in Subwatershed. To develop the hydrological response unit (HRU) in the SWAT model, the slope is essential. It generates from the resolution of 30 m ∗ 30 m DEM for the study area. Slope classification may be single class or multiclass. For this study, the slope option (an option for considering different slope classes for HRU definition) was selected. Therefore, the slope class in this study was classified into four classes. According to [22], slope classification was used to account for lower range in hydrological modelling. Depending on the slope of 0–5%, 5–10%, 10–15%, 15–20%, and >20% were selected for HRU creation of the study Upper Baro Basin. Finally, HRU definition analysis in SWAT helps to load LULC and soil type projects.

2.2.5. Land Use/Land Cover (LU/LC) Analysis. Landsat Satellite images of the years 1987 (Landsat 5), 2002 (Landsat 7) and 2017 (Landsat 8) were obtained from United States Geological Survey (USGS) (https://www.glovis.USGS.gov) (Table 3). The multidate multisensor satellite imagery was collected for successive cropping for each study year. Dataset

Table 3: Landsat data information for the study area.

Reference data	Path/row	Acquisition data	Image	Sensor	Resolution
1987	170/054 170/055 171/054	22/01/1987	Landsat 5	TM	30 m ∗ 30 m
2002	170/054 170/055 171/054	23/01/2002	Landsat 7	ETM+	30 m ∗ 30 m
2017	170/054 170/055 171/054	27/01/2017	Landsat 8	OLF	15 m ∗ 15 m

selections were in dry season fixed with the lowest percent or zero monthly cloud cover. Therefore, all images are cloud-free (0%) in the study area.

The images were already terrain corrected projected to the Universal Transverse Mercator (UTM) of WGS84 zone 37 N. They were radiometrically calibrated to reflectance value and the Quick Atmospheric Correction algorithm was applied in ERDAS software. Radiometric and geometric corrections were applied to the removal of sensor noise, haze, correction data loss, and missing lines due to a solar position, satellite calibration [24, 25]. A supervised image classification method was employed using Maximum Likelihood Algorithm classification. For supervised classification, the Region of Interest (ROI) was made a signature for different LU/LC categories. The reference data collected using a GPS receiver were first converted to a vector file, then the region of interest (ROI) was made in ERDAS software. Using the ROI, the spectral signature of each LU/LC type has been extracted. Further investigations were carried out by taking these sample points in the land use types using a handheld GPS receiver. Based on this analysis and the existing land use distribution information, the area was categorized into eight broad LU/LC classes: cultivated land, woodland, forest land, grazing land, bare land, shrubland, water bodies, and built-up (Table 3).

Overall accuracy and Kappa coefficient, the classify maps will check classification accuracy. According to [26, 27], a good overall classification map accuracy is accepted if and only it possesses an accuracy of at least 85%. The LU/LC was an input of the SWAT model to describe the HRU of the subwatershed. The SWAT Model has predetermined four-letter codes for each LU/LC category (Table 4). These codes were used to link the LU/LC map of the study area with the SWAT land database. To make it compatible, LU/LC with the SWAT model lookup table was prepared for each type of LU/LC.

2.3. SWAT Model Description. SWAT is a physically based semidistributed continuous time-scale hydrological model, which works on a daily time step. This model can simulate runoff, sediment, nutrients, pesticide, and bacterial transport from agricultural watersheds [28]. It simulates the hydrological cycle parameters based on the water balance represented in equation (1) within the watershed [29]. More details on the information about the SWAT model can be found in the SWAT user manual [29].

Table 4: LU/LC class SWAT code.

Value	LU/LC class	SWAT database	SWAT code
1	Forest land	Forest evergreen	FRSE
2	Woodland	Forest-mixed	FRST
3	Grassland	Range-grasses	RNGE
4	Shrubland	Range-brush	RNGB
5	Settlement	Residential-medium density	URMD
6	Agricultural land	Agricultural land-generic	AGRL
7	Bare land	Barren	BARR
8	Waterbody	Water	WATR

The hydrologic cycle simulated by the SWAT is based on the water balance equation [29] as follows:

$$\mathrm{SW}_{t=}\mathrm{SW}_o + \sum_{i=1}^{t}\left[R_i - Q_i - \mathrm{ET}_i - P_i - \mathrm{QR}_i\right], \quad (1)$$

where SW_t and SW_o are the final and initial soil water content, respectively, (mm), Q_i = daily surface runoff (mm), R_i = daily rainfall (mm), ET_i = daily evapotranspiration (mm), R_i = daily lateral flow (mm), and P_i = daily percolation (mm).

2.4. Peak Runoff Rate. The peak runoff rate is a result of the erosive power of a storm and is used to predict sediment loss. SWAT calculates the peak runoff rate with a modified rational method for each HRU using the following equation:

$$Q\mathrm{peak} = \frac{\alpha_{\mathrm{tc}} * Q_{\mathrm{surf}} * A}{t_{\mathrm{conc}}}, \quad (2)$$

where Q peak is peak runoff rate (m^3/s), α_{tc} the fraction of daily rainfall that occurs during the time of concentration, Q_{surf} is the surface runoff (mm), A is the sub-basin area (km^2), and $\mathrm{t}_{\mathrm{conc}}$ is the time of concentration (hr).

2.5. Surface Runoff Generation. The CN method was initially developed for small agricultural watersheds and the CN varies nonlinearly with the moisture content of the soil. It drops to zero as the soil approaches the wilting point and increases to be near 100 as the soil approaches saturation, with higher CNs associated with higher runoff potential watershed. This method is widely used [28].

According to USDA, 1985 [30], this can be mathematically expressed using the following equation:

$$Q_s = \frac{[R_a - I_a]^2}{[R_a - I_a + S]}, \quad \text{For } R_a > I_a,\ Q = 0 \text{ for } R_a \le I_a, \quad (3)$$

where Q_s is the accumulated runoff (mm), Ra is the rainfall depth for the day (mm), and

$$S = 25.4 * \left(\frac{100}{\text{CN}} - 10\right), \quad (4)$$

where CN is the curve number for the day and its value is the function of land use practice, soil permeability and soil hydrologic group. Conceptual framework showing the components and relationships have been used as a framework for the analysis of hydrology in research (Figure 5).

2.6. SWAT Model Simulation, Sensitivity Analysis, Calibration, and Validation. The simulation result cannot be directly used for further analysis. Instead, the ability of the model to sufficiently predict the constituent streamflow should be evaluated through sensitivity analysis, model calibration, and model validation [31].

2.6.1. Sensitivity Analysis. Fifteen hydrological parameters related to streamflow were selected for sensitivity analysis in the study area. The sensitivity of each parameter was identified using the *T* test and *P* values. *P* values were used to determine the significance of the sensitivity. A value close to zero has more significance. *T* test provides a measure of sensitivity and the most sensitive parameters usually appear with *P* values less than the alpha level of 0.05 (larger absolute values are more sensitive) [32].

2.6.2. Model Calibration and Validation. The SUFI-2 algorithm was applied and frequently used in this study of calibration for the SWAT model at a large scale due to its easy application and the reduced number of model runs needed to achieve a decent prediction [33, 34]. In this study, automatic calibration was made every month from January 1, 1990, to December 31, 2002, until the average simulated value came closer to the measured value. Automatic calibration makes use of a numerical algorithm to increase the performance of the model and to optimize the numerical objective functions. After the simulation result for the calibration, the period had fulfilled the above statistical criteria, validation was performed for an independent period of records from January 1, 2003, to December 31, 2009, and the results were compared against an independent set of measured Upper Baro Basin.

2.6.3. Model Performance Evaluation. Model performance was carried out to verify the robustness of the model to simulate hydrological processes. A model performance framework proposed by [35] was used in this study.

Nash and Sutcliffe simulation efficiency (NSE) indicates the degree of fitness of observed and simulated data, and it is calculated using the following equation:

$$\text{NSE} = 1 - \frac{\sum_{i=0}^{N} (Q_{\text{obs}} - Q_{\text{Sim}})^2}{\sum_{i=0}^{N} (Q_{\text{obs}} - \overline{Q}_{\text{obs}})^2}, \quad (5)$$

where N = number of compared values, Q_{obs} is the observed data, $\overline{Q}_{\text{obs}}$ is the observed mean, and Q_{sim} is the simulated data.

The NSE indicates how well the plot of observed versus simulated value fits the 1 : 1 line. The closer the model efficiency is to 1, the more accurate the model, and if it is found between 0 and 1, it indicates deviations between measured and predicted values. If NSE is negative, predictions are poor, and the average value of output is a better estimate than the model prediction [36].

Coefficient of determination (R^2) measures the ability of a model to predict or explain an outcome in the linear regression setting (Equation (6)). R^2 ranges from 0 to 1, with higher values indicating less error variance, and typically values greater than 0.5 are considered acceptable [35, 37, 38].

$$R^2 = \frac{\sum (X_i - X_{\text{av}})(Y_i - Y_{\text{av}})}{\sqrt{\sum \left(X_{i-X_{\text{av}}}\right)^2} \sqrt{\sum \left(Y_{i-Y_{\text{av}}}\right)^2}}, \quad (6)$$

where X_i is measured value, X_{av} is average measured value, Y_i is simulated value, and Y_{av} is the average simulated value.

Percent bias (PBIAS) measures the average difference between the simulated and measured values for a given quantity over a specified period (usually the entire calibration or validation period) and it is calculated using the following equation [39, 40]:

$$\text{PBIAS} = \left[\frac{\sum Y_i - \sum X_i}{X_i}\right], \quad (7)$$

where X_i is measured value and Y_i is simulated value.

Model evaluation classifies as follows:

(i) $0.75 < \text{NSE} < 1.00$, $\text{PBIAS} < \pm 10$—better predictor

(ii) $0.65 < \text{NSE} \le 0.75$, $\pm 10 < \text{PBIAS} < \pm 15$—good

(iii) $0.50 < \text{NSE} \le 0.65$, $\pm 15 < \text{PBIAS} < \pm 25$—satisfactory

(iv) ($\text{NSE} \le 0.50$, $\text{PBIAS} > \pm 25$)—unsatisfactory

3. Results and Discussion

3.1. LU/LC Change. The spatial distribution and percentage of the total area of the eight LU/LC types between 1987–2002, 2002–2017, and 1987–2017 are shown in Figure 6 (Table 5).

The results obtained for 1987–2002 reveal that *forest land covers* 36.74% and followed by grassland, 19.77% and shrubland and woodland also cover 19.76% and 11.32%, respectively. Between 2002 and 2017, the distribution of forest cover demonstrates highest in the catchment, which covered 33.33%, followed by agricultural land and shrubland, with the value of 15.6%, 15.1%, respectively. *Forest land* and shrubland decreased after 1987–2002, with −3.41% and −4.65%, respectively (Figure 7). The area of *forest land decreased* due to of change of land use (conversion) to the expansion of agricultural land in the southwestern part of

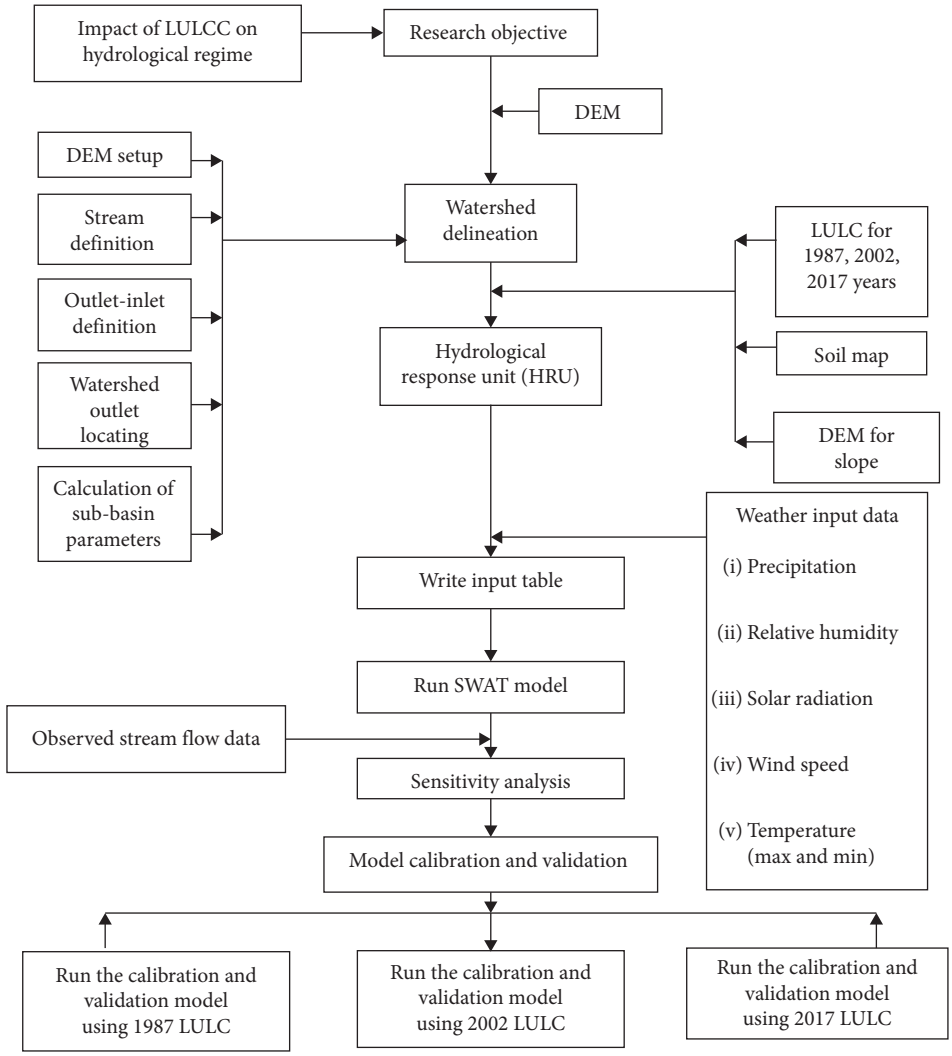

Figure 5: General conceptual methodology used for modelling hydrology in the Upper Baro Basin.

the catchment. The urban area gradually expanded from 2.01% to 15.51% over the entire study period. These results indicate that government policy does not have a strong impact on land use.

In the last 30 years, the study displays an increase in agriculture, bare land, urban, and shrubland, whereas the forest, grassland, water, and wetland were noted declined. Agricultural land increased by 18.01% during the study period. This is due to the increase of population growth that causes the increase in demand for cultivation land for different agricultural products like cereal crops, field crops, industrial crops, whereas the forest area was diminished. This might be due to deforestation activities that have taken place for agriculture and urban expansion.

Consequently, agricultural investment policies encouraged further deforestation that leads to land conversion [41] and various types of natural forests and woodlands in the Western part of Ethiopia, being cleared and replaced by commercial agriculture [42, 43]. In the study basin, cultivated land has gained/increased by 18.01%, mainly converted from the grazing land by 15.64%. Forest and shrubland conversion also contributed to the increasing cultivated land.

In this study, the accuracy assessment was performed using the 340 referenced points collected through stratified sampling. Overall accuracies obtained were 92.14%, 94.63%, and 95.93% for the 1987, 2002, and 2017 images, respectively (Table 6). The overall accuracy was computed by dividing the correct classification by the total number of reference pixels in the error matrix.

3.2. Stream Flow Modeling Using SWAT

3.2.1. Sensitivity Analysis. Sensitivity analysis was carried out to identify which model parameter was the most important or sensitive. Flow sensitivity analysis was carried out for 13 years, the calibration period (from January 1, 1990, to December 31, 2002). The default and optimal parameters and their ranking in terms of the 10 highest relative sensitivity values used to develop, calibrate, and validate the model (Figure 8).

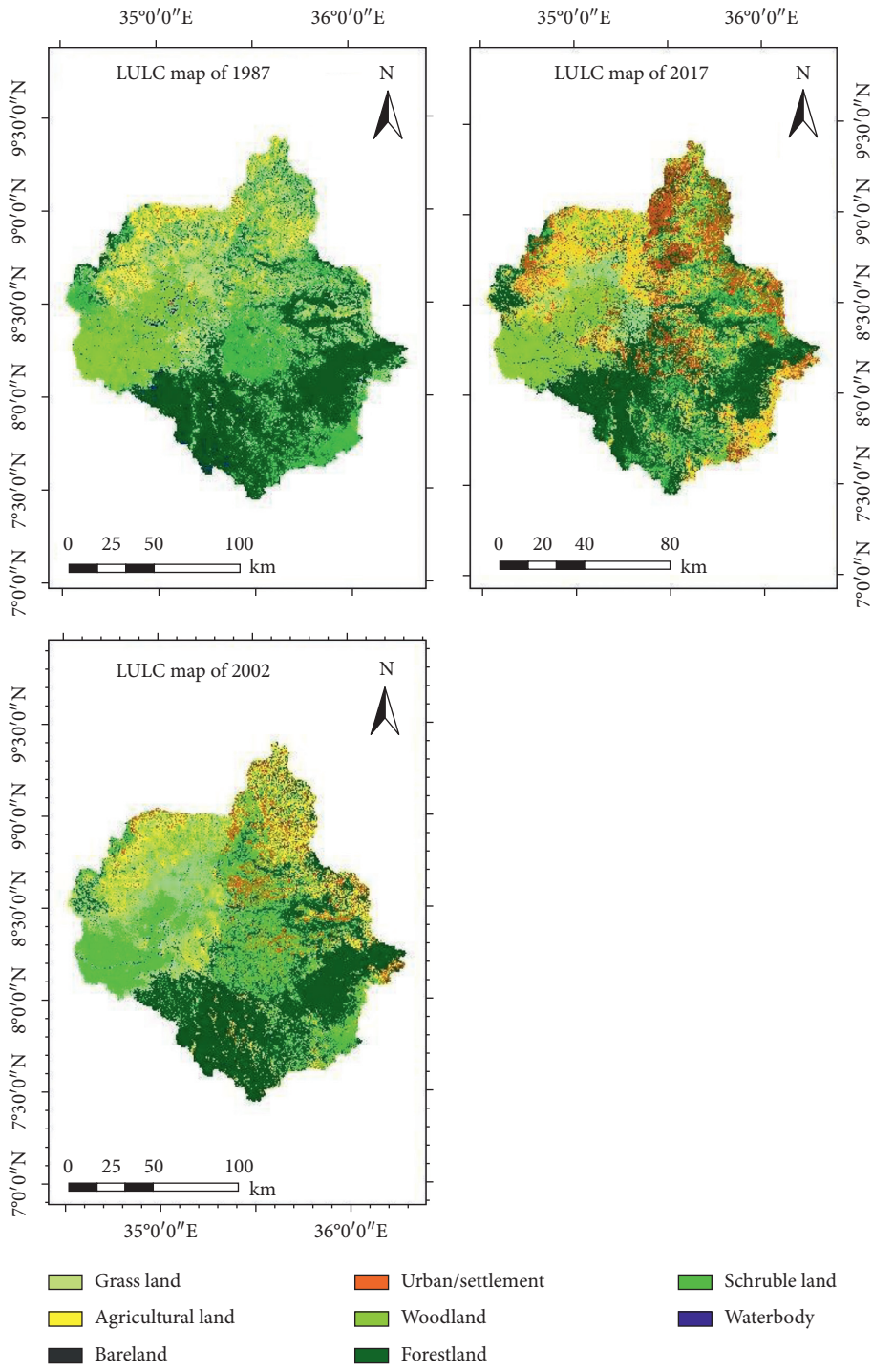

Figure 6: Land use land cover map of 1987, 2002, and 2017.

3.2.2. SWAT Model Calibration and Validation. The simulated monthly flows demonstrated a good agreement with the monthly observed discharge of Upper Baro Basin with a coefficient of determination ($R^2 = 0.86$), Nash–Sutcliffe efficiency (NSE = 0.80), and percent bias (PBIAS = −17%) (Figure 9). However, the model overestimated the peak monthly flow for some years in the calibration period; it followed the trend of observed monthly Upper Baro basin discharge and presented a good response to extreme rainfall events, which resulted in high runoff volume.

SWAT model also successfully validated streamflow for an independent period (2003–2010) with $R^2 = 0.84$, NS = 0.76, and PBIAS = −4.5% during the validation period; the values fulfilled the statistical model performance criteria $R^2 > 0.6$ and NSE > 0.5 recommended by SWAT developer [37]. The percent bias (PBAIS) values (−17% and 4.5%)

Table 5: The magnitude of land use/land cover type for 1987, 2002, and 2017 in the Upper Baro Basin.

Land use class	Spatial converge						Change between years					
	1987		2002		2017		2002–1987		2017–2002		2017–1987	
	(km^2)	%	(km^2)	%	(km^2)	%	(km^2)	%	(km^2)	%	(km^2)	%
Grass land	4639.21	19.77	3272.15	13.95	969.34	4.13	−1367.05	−5.83	−2302.81	−9.82	−3669.87	−15.64
Agricultural	2065.92	8.81	3659.08	15.60	6290.56	26.81	1593.15	6.79	2631.48	11.22	4224.63	18.01
Bare land	92.81	0.40	166.24	0.71	217.43	0.93	73.43	0.31	51.19	0.22	124.62	0.53
Urban	471.30	2.01	2060.52	8.78	3638.16	15.51	1589.23	6.77	1577.64	6.72	3166.86	13.50
Woodland	2656.81	11.32	2812.80	11.99	2,447.74	10.43	155.98	0.66	−365.06	−1.56	−209.08	−0.89
Forestland	8619.97	36.74	7819.91	33.33	7323.35	31.21	−800.06	−3.41	-496.56	−2.12	−1296.62	−5.53
Schruble land	4635.94	19.76	3544.63	15.11	2393.95	10.20	−1091.31	−4.65	−1150.69	−4.90	−2241.99	−9.56
Waterbody	280.04	1.19	126.66	0.54	81.48	0.35	−153.37	−0.65	−45.18	−0.19	−198.56	−0.85

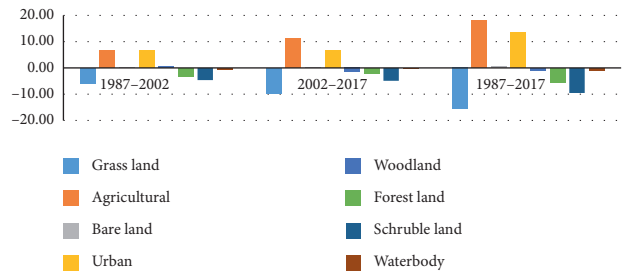

Figure 7: Comparison of LULC classes of the years 1987–2002, 2002–2017, and 1987–2017.

Table 6: Confusion matrix for classified images.

LU/LC class	1987		2002		2017	
	producer	User	Producer	User	Producer	User
Forest land (FT)	97	95.59	96.08	98	100	96.61
Woodland (WD)	95	93.44	97.44	100	96.15	100
Grass land (GR)	81.01	83.33	93.55	90.63	92.16	94
Urban (UB)	87.5	93.33	95.74	84.91	100	88
Shrub land (SL)	91.67	93.62	100	93.88	100	100
Agriculture (AG)	92.11	89.74	86.54	91.84	91.07	92.73
Waterbody (WB)	100	100	97.44	100	100	100
Bare land (BL)	90.24	86.05	91.84	100	87.1	100
Overall accuracy	92.14%		94.63		95.93	
Kappa coefficient	0.9094		0.9385		0.9533	

during calibration and validation periods, respectively, also fulfilled the statistical model performance criteria PBAIS> ±15 [35] (Table 7).

The percentage of observations bracketed by the 95 PPU was 75% for calibration and 72% for validation. The r-factor, which is the average thickness of the 95PPU band divided by the standard deviation of the measured data, was 1.08 for calibration and 0.84 for validation. According to [32], a p-factor greater than 0.70 and r-factor less than 1.5 display that the model is accurate in simulating streamflow. Thus, the results displayed that the model accurately simulated the biophysical processes influencing flow in the study area.

Generally, the above information showed that the performance of the model was better during the calibration period more than the validation period (Table 8) and also the calibration validation period (Figures 9–12) shows there was good relation with observed and simulated streamflow.

3.3. Land Use/Land Cover Change Response to Hydrological Process. The simulated results of the Upper Baro Basin under different land use/land cover scenarios are shown in Table 9.

3.4. Mean Monthly Wet and Dry Month Streamflow Simulation and Their Variability. Months July, August, and September were considered as wet periods and Jan, Feb, and March were considered dry months; these seasonal variabilities of streamflow were evaluated.

3.5. Spatial Variability of Surface Runoff over Sub-Basin. Spatial variability of surface runoff shows that surface runoff is highly sensitive to the change of LU/LC over sub-watersheds in the period of 1987, 2002, and 2017 (Figure 13).

3.6. Comparison of Mean Monthly Surface Runoff and Groundwater. Decreases in base flow had a potential effect on the change in annual river flow (Figure 14). Results from LU/LC change scenarios, the mean monthly (wet and dry) flow has increased from 82.9 mm and decreased 20.54 mm concerning the change of LU/LC from 1987 to 2017 (Figure 15).

The results (Table 10) demonstrate that the mean dry monthly flow for 1987–2017 land cover decreased by −20.54 (m^3/s) when compared to the land cover in 1987–2017. Changes in land use occurred in all parts of the Basin but mainly in the southwestern part. Vegetation cover within the catchment had changed considerably due to human activities, mainly through the conversion of natural vegetation to agriculture, Urban, and largescale investment. These changes have altered water resources through biophysical and biogeochemical processes in the soil. Through these land-cover changes, the biophysical and morphological

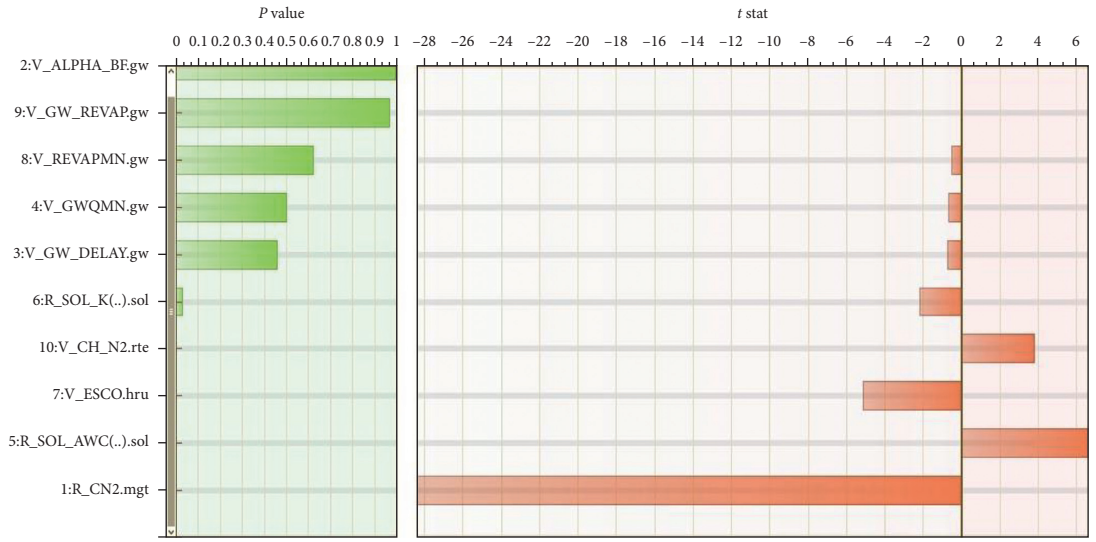

Figure 8: Global sensitivity analysis for streamflow.

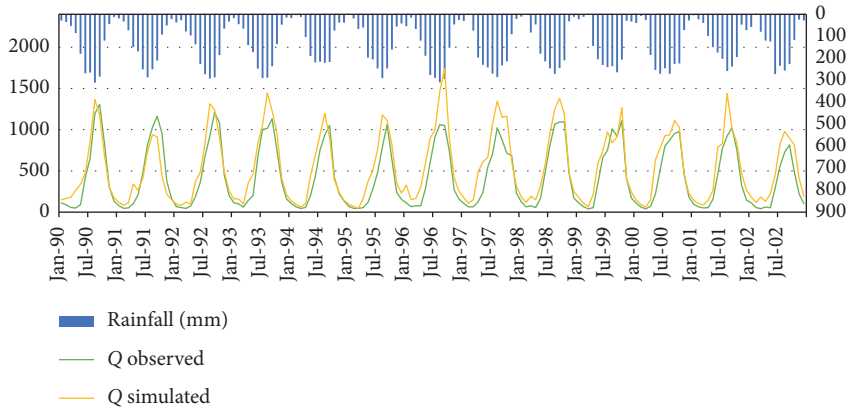

Figure 9: Calibration of average monthly observed and simulated flow (1990–2002).

Table 7: Result of final calibrated flow parameters for Upper Baro Basin.

Parameter name	Fitted value	Range
R_CN2	−0.230	±0.25
V_ALPHA_BF	0.053	0-1
V_GW_DELAY	113.50	0–500
V_GW_REVAP	0.1343	0.02–0.2
V_CH_N2	0.3436	0.01–1
R_SOL_K	0.5450	0-1
R_SOL_AWC	0.755	0-1
V_ESCO.hru	0.2530	0-1
V_REVAPMN.gw	0.3700	0–10
V_GWQMN.gw	1.982	0–2

Table 8: Summary of model performance evaluation for calibration and validation period on monthly time steps.

Period	Mean annual water yield (m^3/s)		Monthly model efficiency measures		
	Observed	Simulated	R^2	NSE	PBAIS (%)
Calibration	422.461	535.96	0.86	0.81	−18.7
Validation	374.42	451.12	0.84	0.76	−19.8

characteristics of the vegetation have been modified, and therefore, the changes have affected the exchange of water between the atmosphere and land surface. Similarly, the results indicate an increase in surface runoff increased from 773 mm/yr in 1987 to 793.05 mm/yr in 2002 and 816.53 mm/yr in 2017 due to a drastic increase in agriculture and urban activity at the expense of other land covers while groundwater was decreased from 283.21 mm to 257.13 mm in 1987 as compared to 2017 due to LULC change. Similarly, [44, 45] reported that an increase in annual surface runoff increased when forest lands were converted to the other classes especially cultivated land. The expansion of agricultural land by displacing forest and shrubland results in an increase in surface erosion generation following rainfall events and causes a reduction in soil moisture conditions and groundwater recharge to shallow aquifers. Similarly, studies suggested that grassland and lateral flow are positively correlated [46, 47].

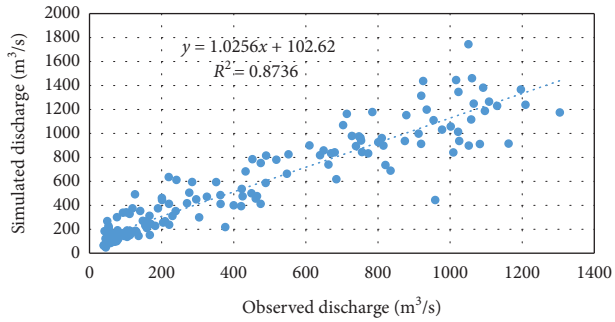

Figure 10: Simulated versus observed monthly flow for calibration (1990–2002).

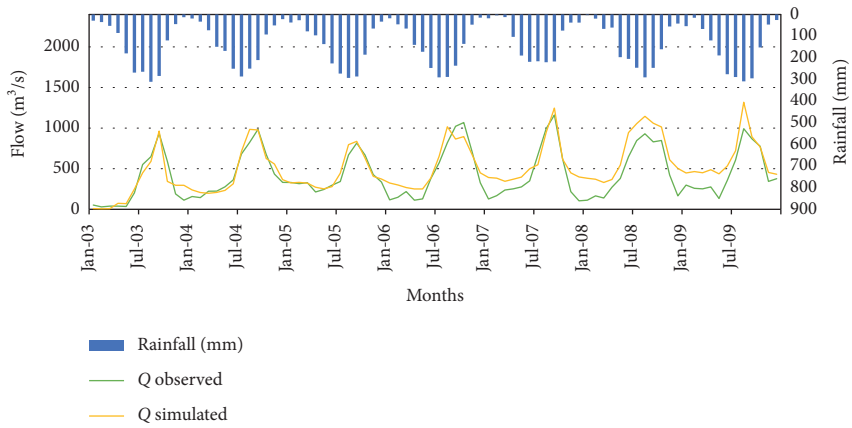

Figure 11: Validation of average monthly observed and simulated flow (2003–2009).

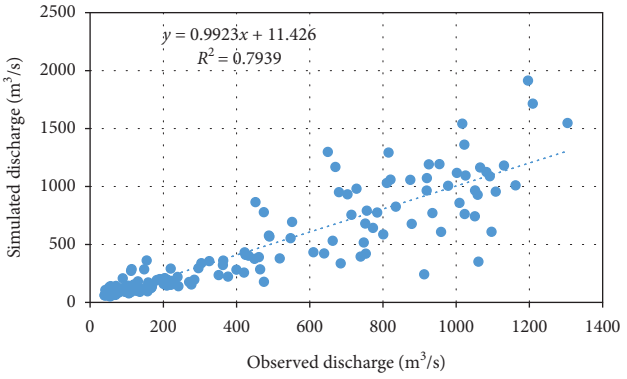

Figure 12: Simulated versus observed monthly flow for calibration (2003–2009).

Table 9: Average annual hydrological summaries under different LULC.

Parameter	LU/LC 1987 (mm)	LU/LC 2002 (mm)	LU/LC 2017 (mm)	Change detection		
				1987–2002	2002–2017	1987–2017
SUR Q	773.	793.05	816.53	20.05	23.48	43.53
GW Q	270.8	259.29	243.22	−11.08	−16.07	−27.58
LAT Q	87.37	85.49	81.74	−1.88	−3.75	−5.63
WYLD	1131.71	1137.83	1141.49	6.12	3.66	9.78
PERC	302.62	291.17	275.00	−11.45	−16.17	−27.62
ET	807.1	800.4	797	−6.7	−3.4	−10.1
SEDI	62.72	106.02	124.49	43.3	18.47	61.77
CN	76.89	77.83	78.82			

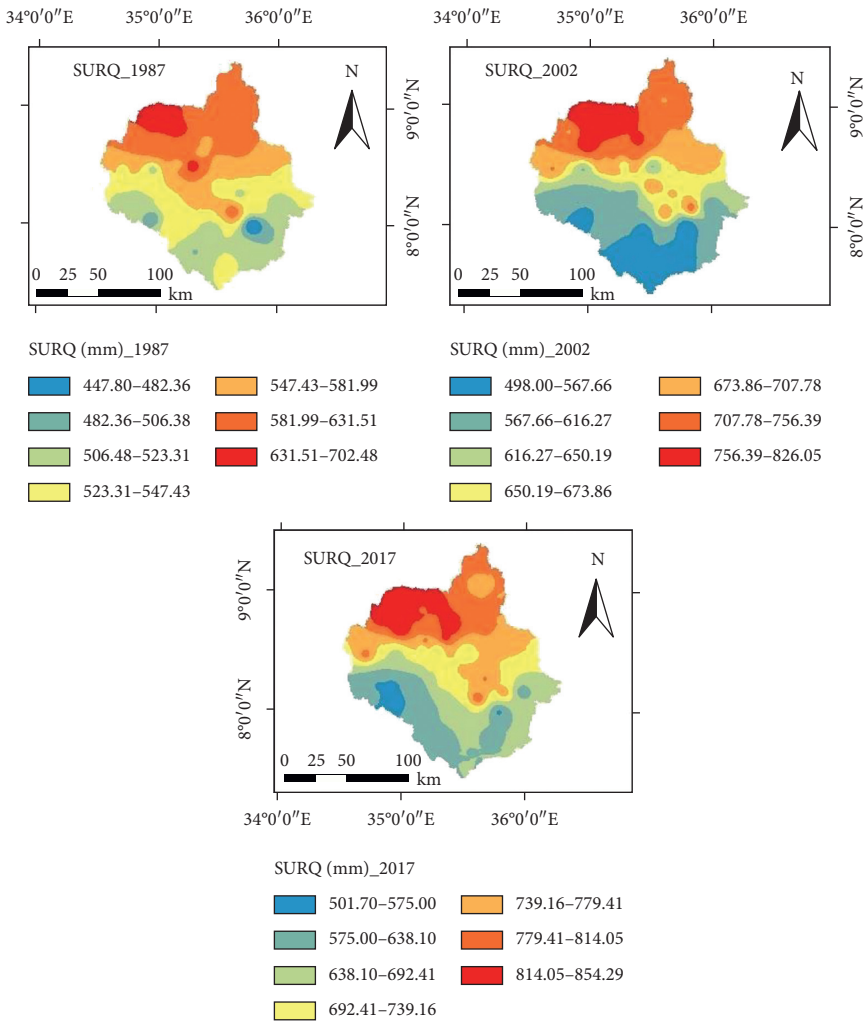

Figure 13: Spatial distribution predicted annual surface runoff (SURQ) (mm) for different LULC conditions.

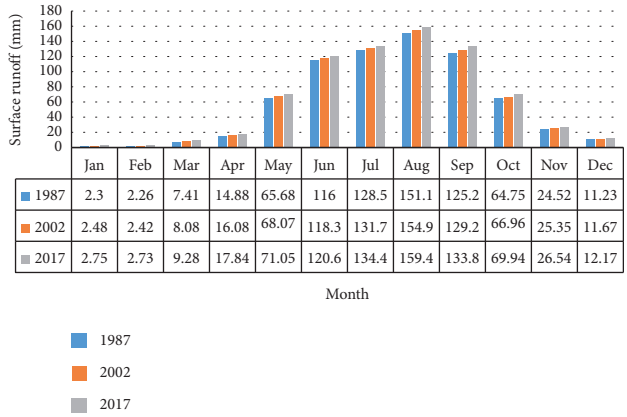

	Jan	Feb	Mar	Apr	May	Jun	Jul	Aug	Sep	Oct	Nov	Dec
1987	2.3	2.26	7.41	14.88	65.68	116	128.5	151.1	125.2	64.75	24.52	11.23
2002	2.48	2.42	8.08	16.08	68.07	118.3	131.7	154.9	129.2	66.96	25.35	11.67
2017	2.75	2.73	9.28	17.84	71.05	120.6	134.4	159.4	133.8	69.94	26.54	12.17

Figure 14: Mean monthly surface runoff (mm).

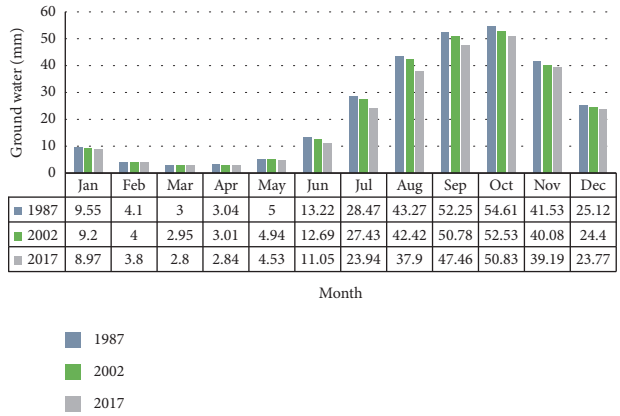

	Jan	Feb	Mar	Apr	May	Jun	Jul	Aug	Sep	Oct	Nov	Dec
1987	9.55	4.1	3	3.04	5	13.22	28.47	43.27	52.25	54.61	41.53	25.12
2002	9.2	4	2.95	3.01	4.94	12.69	27.43	42.42	50.78	52.53	40.08	24.4
2017	8.97	3.8	2.8	2.84	4.53	11.05	23.94	37.9	47.46	50.83	39.19	23.77

Figure 15: Mean monthly groundwater recharge (mm).

Table 10: Mean monthly wet and dry month streamflow simulation and their variability.

Mean monthly streamflow (m^3/s)						Mean monthly streamflow change					
1987		2002		2017		2002–1987		2017–2002		2017–1987	
Dry	Wet	Dry	Wet	Dry	Wet	Dry	Wet	Dry	Wet	Dry	Wet
84.2	871.2	72.15	907	63.66	954.1	−12.05	+35.8	−8.49	+47.1	−20.54	+82.9

4. Conclusions

In the present study, the Upper Baro Basin has been simulated using the SWAT hydrological model for assessing the impact of LULC change on its hydrological regime successfully. Initially, the change in LULC between the years 1987, 2002, and 2017 has been assessed. It is evident that land cover changes had occurred between 1987 and 2017. Forest cover had decreased from 36.74% to 31.21%, attributable to logging for timber, firewood, and clearing for agricultural purposes. In contrast, the agricultural area increased over the years from 8.81% to 26.81%. Similarly, grasslands and bushes have also been converted to agricultural areas. Sensitivity analysis of the SWAT parameters indicates that runoff is most sensitive to curve number, an available water capacity of the soil layer, soil evaporation composition factor, manning's "*n*" value for the main channel, and saturated hydraulic conductivity. Seasonal streamflow variability due to the LU/LC was assessed and comparisons were made on surface runoff, lateral flow, and groundwater flow contributions to streamflow based on the three simulation outputs. Surface runoff was increased from 713.85 mm to 760.49 mm, while groundwater was decreased from 283.21 mm to 257.13 mm in the years 1987 and 2017. Also, surface runoff was increased from 737.67 mm to 760.49 mm, while groundwater was decreased from 266.32 mm to 257.13 mm in the year 2002 and 2017. Land use/land cover change over the last 30 years also affect the soil and soil properties in the study area significantly. For example, forest land declined and agricultural land is increased. This dynamism would maximize soil erosion, which leads to the loss of important soil nutrients. Therefore, different soil and water conservation measures are required to reverse the challenges.

Data Availability

The data used to support the findings of this study are available from the corresponding author upon request.

Conflicts of Interest

The authors declare that they have no conflicts of interest.

References

[1] V. Garg, B. R. Nikam, P. K. Thakur, S. P. Aggarwal, P. K. Gupta, and S. K. Srivastav, "Human-induced land use land cover change and its impact on hydrology," *HydroResearch*, vol. 1, pp. 48–56, 2019.

[2] Y. Li, J. Chang, L. Luo et al., "Spatiotemporal impacts of land use land cover changes on hydrology from the mechanism perspective using SWAT model with time-varying parameters," *Hydrology Research*, vol. 50, no. 1, pp. 244–261, 2019.

[3] H. Brook, M. Argaw, H. Sulaiman, and T. A. Abiye, "The impact of land use/land cover change on hydrological components due to resettlement activity: SWAT model approach," *International Journal of Ecology and Environmental Sciences*, vol. 37, pp. 49–60, 2015.

[4] R. E. Schulze, "Modelling hydrological responses to land use and climate change: a southern african perspective," *AMBIO: A Journal of the Human Environment*, vol. 29, no. 1, pp. 12–22, 2000.

[5] T. J. Stohlgren, T. N. Chase, R. A. Pielke, T. G. F. Kittel, and J. S. Baron, "Evidence that local land use practices influence regional climate, vegetation, and stream flow patterns in adjacent natural areas," *Global Change Biology*, vol. 4, pp. 495–504, 1998.

[6] N. Marie Mireille, H. M. Mwangi, J. K. Mwangi, and J. Mwangi Gathenya, "Analysis of land use change and its impact on the hydrology of kakia and esamburmbur sub-

watersheds of Narok county, Kenya," *Hydrology*, vol. 6, no. 4, p. 86, 2019.

[7] S. Babar and H. Ramesh, "Streamflow response to land use-land cover change over the nethravathi river Basin, India," *Journal of Hydrologic Engineering*, vol. 20, no. 10, 2015.

[8] Food and Agriculture Organization, "World reference base for soil resources 2014, international soil classification system for naming soils and creating legends for soil maps," World Soil Resources Report 106, Food and Agriculture Organization, Rome, Italy, 2014.

[9] D. F. Tufa, Y. Abbulu, and G. Srinivasarao, "Watershed hydrological response to changes in land use/land covers patterns of river basin: a review," *International Journal of Civil, Structural, Environmental and Infrastructure Engineering Research and Development (IJCSEIERD)*, vol. 4, pp. 157–170, 2014.

[10] A. B. Dixon, "The hydrological impacts and sustainability of wetland drainage cultivation in Illubabor, Ethiopia," *Land Degradation & Development*, vol. 13, no. 1, pp. 17–31, 2002.

[11] T. Gashaw, T. Tulu, M. Argaw, and A. W. Worqlul, "Modeling the hydrological impacts of land use/land cover changes in the Andassa watershed, Blue Nile Basin, Ethiopia," *Science of the Total Environment*, vol. 619-620, pp. 1394–1408, 2018.

[12] V. Garg, S. P. Aggarwal, P. K. Gupta et al., "Assessment of land use land cover change impact on hydrological regime of a basin," *Environmental Earth Sciences*, vol. 76, no. 18, p. 635, 2017.

[13] G. Shao, Y. Guan, D. Zhang, B. Yu, and J. Zhu, "The impacts of climate variability and land use change on streamflow in the Hailiutu River Basin," *Water*, vol. 10, no. 6, p. 814, 2018.

[14] L. Zhang, R. Karthikeyan, Z. Bai, and R. Srinivasan, "Analysis of streamflow responses to climate variability and land use change in the Loess Plateau region of China," *Catena*, vol. 154, pp. 1–11, 2017.

[15] P. Sun, Y. Wu, X. Wei et al., "Quantifying the contributions of climate variation, land use change, and engineering measures for dramatic reduction in streamflow and sediment in a typical loess watershed, China," *Ecological Engineering*, vol. 142, Article ID 105611, 2020.

[16] A. A. Vaighan, N. Talebbeydokhti, and A. M. Bavani, "Assessing the impacts of climate and land use change on streamflow, water quality and suspended sediment in the Kor River Basin, southwest of Iran," *Environmental Earth Sciences*, vol. 76, p. 543, 2017.

[17] Y. S. Getahun and H. Van Lanen, "Assessing the impacts of land use-cover change on hydrology of Melka Kuntrie sub-basin in Ethiopia, using a conceptual hydrological model," *Hydrology: Current Research*, vol. 6, no. 3, pp. 1–11, 2015.

[18] T. Karvonen, H. Koivusalo, M. Jauhiainen, J. Palko, and K. Weppling, "A hydrological model for predicting runoff from different land use areas," *Journal of Hydrology*, vol. 217, no. 3-4, pp. 253–265, 1999.

[19] M. Wegehenkel, "Estimating of the impact of land use changes using the conceptual hydrological model THESEUS––a case study," *Physics and Chemistry of the Earth, Parts A/B/C*, vol. 27, pp. 631–640, 2002.

[20] H. E. Getachew and A. M. Melesse, "The impact of land use change on the hydrology of the Angereb watershed, Ethiopia," *International Journal of Water Sciences*, vol. 1, 2012.

[21] D. Legesse, T. Abiye, C. Vallet-Coulomb, and H. Abate, "Streamflow sensitivity to climate and land cover changes: Meki River, Ethiopia," *Hydrology and Earth System Sciences*, vol. 14, no. 11, 2010.

[22] S. G. Setegn, R. Srinivasan, and B. Dargahi, "Hydrological modelling in the lake Tana Basin, Ethiopia using SWAT model," *The Open Hydrology Journal*, vol. 2, no. 1, pp. 49–62, 2008.

[23] G. Zeleke and H. Hurni, "Implications of land use and land cover dynamics for mountain resource degradation in the Northwestern Ethiopian highlands," *Mountain Research and Development*, vol. 21, pp. 184–191, 2001.

[24] T. Hilker, A. I. Lyapustin, C. J. Tucker, P. J. Sellers, F. G. Hall, and Y. Wang, "Remote sensing of tropical ecosystems: atmospheric correction and cloud masking matter," *Remote Sensing of Environment*, vol. 127, pp. 370–384, 2012.

[25] A. I. Lyapustin, Y. Wang, I. Laszlo et al., "Multi-angle implementation of atmospheric correction for MODIS (MAIAC): 3. atmospheric correction," *Remote Sensing of Environment*, vol. 127, pp. 385–393, 2012.

[26] J. R. Anderson, *A Land Use and Land Cover Classification System for Use with Remote Sensor Data*, US Government Printing Office, Washington, DC, USA, 1976.

[27] G. M. Foody, "Status of land cover classification accuracy assessment," *Remote Sensing of Environment*, vol. 80, no. 1, pp. 185–201, 2002.

[28] J. G. Arnold, R. Srinivasan, R. S. Muttiah, and J. R. Williams, "Large area hydrologic modeling and assessment part I: model development," *Journal of the American Water Resources Association*, vol. 34, no. 1, pp. 73–89, 1998.

[29] S. L. Neitsch, J. G. Arnold, J. R. Kiniry, and J. R. Williams, *Soil and Water Assessment Tool Theoretical Documentation Version 2009*, Texas Water Resources Institute, Austin, TX, USA, 2011.

[30] "United State Department of Agriculture - Soil Conservation Service (USDA-SCS)," *National Engineering Handbook*, USDA, Washington, DC, USA, 1985.

[31] K. L. White and I. Chaubey, "Sensitivity analysis, calibration, and validations for a multisite and multivariable SWAT model 1," *JAWRA Journal of the American Water Resources Association*, vol. 41, pp. 1077–1089, 2005.

[32] K. C. Abbaspour, E. Rouholahnejad, S. Vaghefi, R. Srinivasan, H. Yang, and B. Kløve, "A continental-scale hydrology and water quality model for Europe: calibration and uncertainty of a high-resolution large-scale SWAT model," *Journal of Hydrology*, vol. 524, pp. 733–752, 2015.

[33] K. C. Abbaspour, *SWAT-CUP 2012. SWAT Calibration and Uncertainty Program—A User Manual*, Swiss Federal Institute of Aquatic Science and Technology, Dübendorf, Switzerland, 2013.

[34] B. Narsimlu, A. K. Gosain, B. R. Chahar, S. K. Singh, and P. K. Srivastava, "SWAT model calibration and uncertainty analysis for streamflow prediction in the Kunwari River Basin, India, using sequential uncertainty fitting," *Environmental Processes*, vol. 2, no. 1, pp. 79–95, 2015.

[35] D. N. Moriasi, J. G. Arnold, M. W. Van Liew, R. L. Bingner, R. D. Harmel, and T. L. Veith, "Model evaluation guidelines for systematic quantification of accuracy in watershed simulations," *Transactions of the ASABE*, vol. 50, no. 3, pp. 885–900, 2007.

[36] J. E. Nash and J. V. Sutcliffe, "River flow forecasting through conceptual models part I—a discussion of principles," *Journal of Hydrology*, vol. 10, no. 3, pp. 282–290, 1970.

[37] C. Santhi, J. G. Arnold, J. R. Williams, W. A. Dugas, R. Srinivasan, and L. M. Hauck, "Validation of the swat model on a large river Basin with point and nonpoint sources," *Journal of the American Water Resources Association*, vol. 37, no. 5, pp. 1169–1188, 2001.

[38] M. Van Liew, J. Arnold, and J. Garbrecht, "Hydrologic simulation on agricultural watersheds: choosing between two models," *Transactions of the ASAE*, vol. 46, p. 1539, 2003.

[39] H. V. Gupta, S. Sorooshian, and P. O. Yapo, "Status of automatic calibration for hydrologic models: comparison with multilevel expert calibration," *Journal of Hydrologic Engineering*, vol. 4, no. 2, pp. 135–143, 1999.

[40] P. Shi, C. Chen, R. Srinivasan et al., "Evaluating the SWAT model for hydrological modeling in the Xixian watershed and a comparison with the XAJ model," *Water Resources Management*, vol. 25, no. 10, pp. 2595–2612, 2011.

[41] S. Gebreselassie, "Intensification of smallholder agriculture in Ethiopia: options and scenarios," *Future Agricultures Consortium Meeting at the Institute of Development Studies*, pp. 20–22, 2006.

[42] A. K. Gobena and T. Y. Gan, "Incorporation of seasonal climate forecasts in the ensemble streamflow prediction system," *Journal of Hydrology*, vol. 385, no. 1–4, pp. 336–352, 2010.

[43] E. N. Stebek, "Between "land grabs" and agricultural investment: land rent contracts with foreign investors and Ethiopia's normative setting in focus," *Mizan Law Review*, vol. 5, pp. 175–214, 2011.

[44] L. A. Anaba, N. Banadda, N. Kiggundu, J. Wanyama, B. Engel, and D. Moriasi, "Application of SWAT to assess the effects of land use change in the murchison bay catchment in Uganda," *Computational Water, Energy, and Environmental Engineering*, vol. 6, no. 1, pp. 24–40, 2017.

[45] T. S. Ngo, D. B. Nguyen, and P. S. Rajendra, "Effect of land use change on runoff and sediment yield in da river basin of Hoa Binh province, northwest Vietnam," *Journal of Mountain Science*, vol. 12, no. 4, pp. 1051–1064, 2015.

[46] C. Gyamfi, J. Ndambuki, and R. Salim, "Hydrological responses to land use/cover changes in the Olifants Basin, South Africa," *Water*, vol. 8, no. 12, p. 588, 2016.

[47] S. Shukla and S. Gedam, "Evaluating hydrological responses to urbanization in a tropical River Basin: a water resources management perspective," *Natural Resources Research*, vol. 28, no. 2, pp. 327–347, 2019.